

Probability distributions of radiocarbon in open compartmental systems

Ingrid Chanca¹, Susan Trumbore¹, Kita Macario², and Carlos A. Sierra³

¹Max Planck Institute for Biogeochemistry

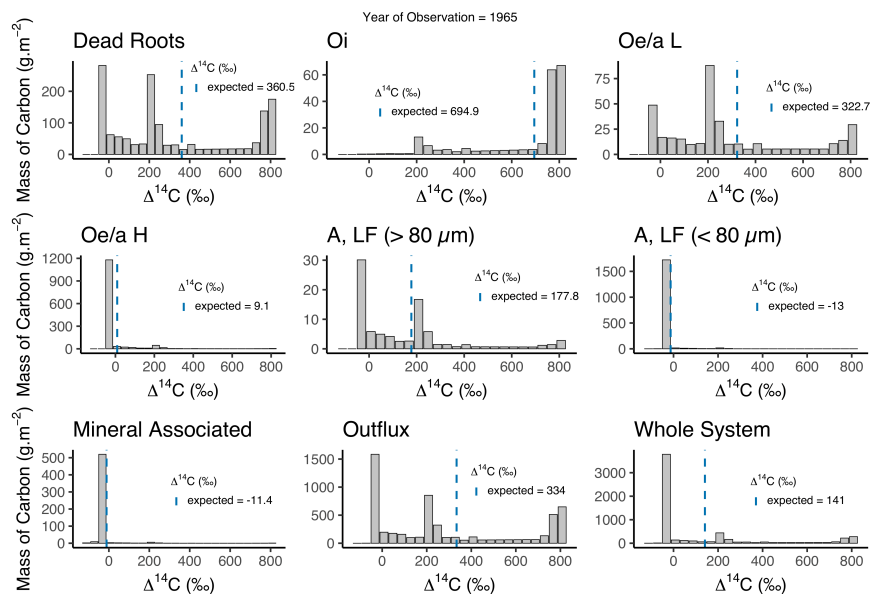
²Universidade Federal Fluminense

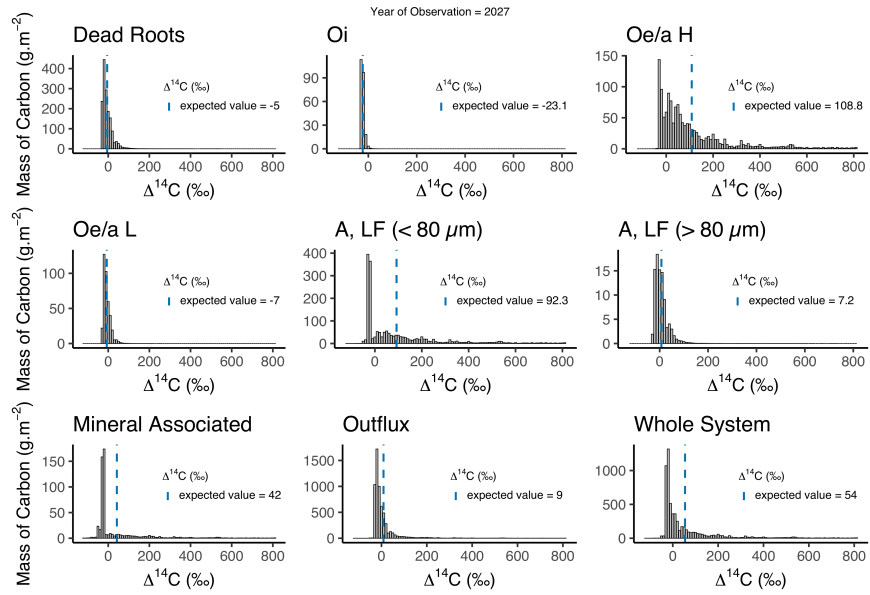
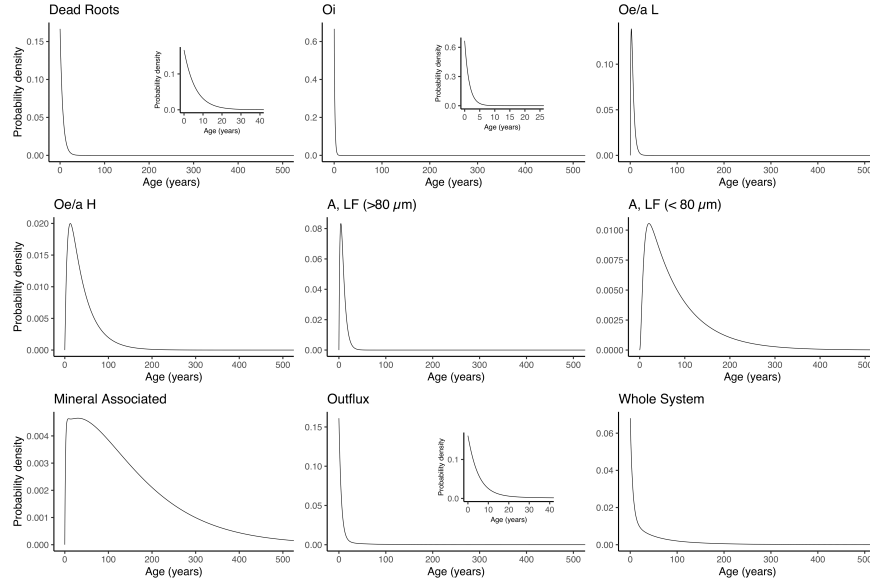
³Max-Planck-Institute for Biogeochemistry

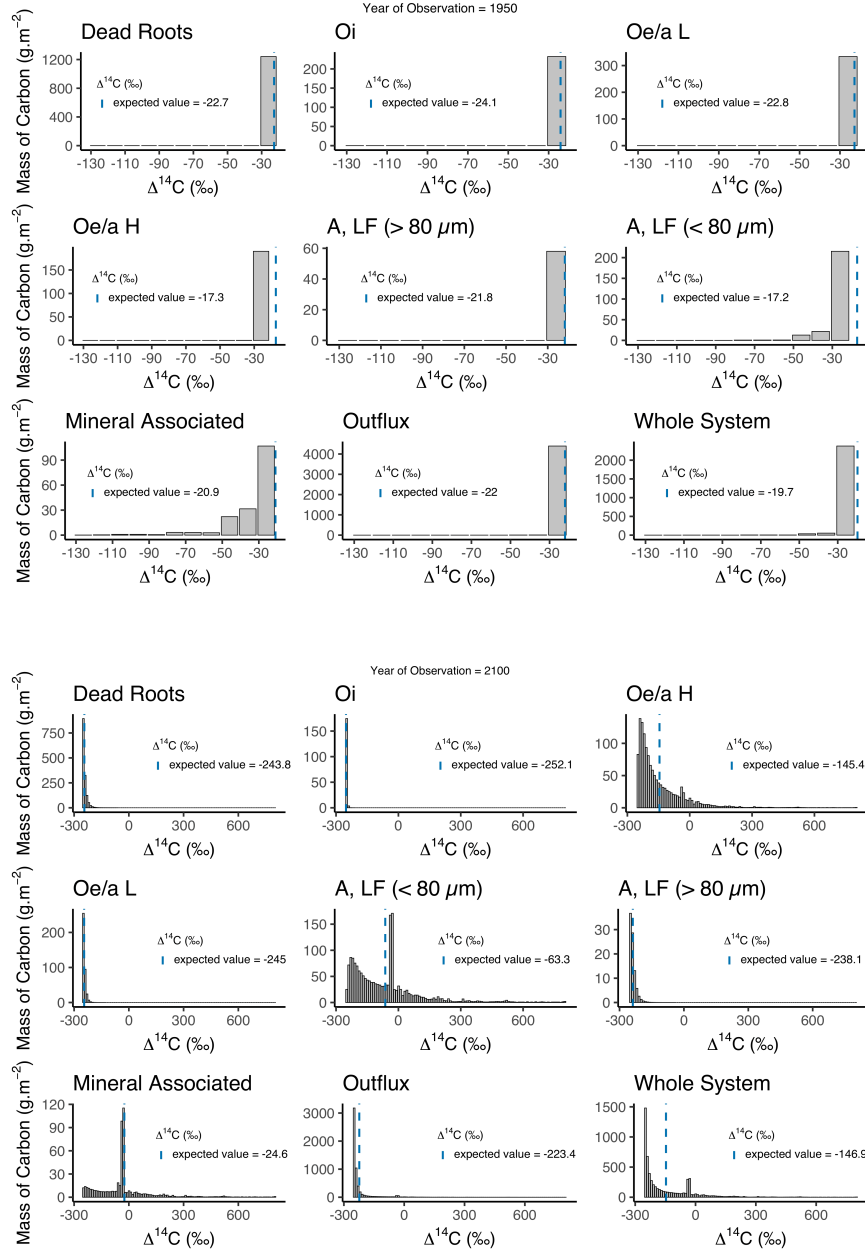
November 26, 2022

Abstract

Radiocarbon (^{14}C) is commonly used as a tracer of the carbon cycle to determine how fast carbon moves between different reservoirs such as plants, soils, rivers or oceans. However such studies mostly emphasize the mean value (as $\Delta^{14}\text{C}$) of an unknown probability distribution. We introduce a novel algorithm to compute $\Delta^{14}\text{C}$ distributions from knowledge of the age distribution of carbon in compartmental systems at equilibrium. Our results demonstrate that the shape of the distributions might differ according to the speed of cycling of ecosystem compartments and their connectivity within the system, and are mostly non-normal. The distributions are also sensitive to the variations of $\Delta^{14}\text{C}$ in the atmosphere over time, as influenced by the counteracting anthropogenic effects of fossil-fuel emissions (^{14}C -free) and nuclear weapons testing (bomb ^{14}C). Lastly, we discuss insights that such distributions can offer for sampling and design of experiments aiming to capture the precise variability of $\Delta^{14}\text{C}$ values in ecosystems.







1 r b a b i l i d i r i b u i r a d i c a r b o n i n e
2 c a r b o n e a r t h e

3 1 2 1 2 A 1 3

4 ¹MaxPlanck-Institut für Biogeochemie, Hans-Köll-Str. 10, Jena, Germany

5 ²Laboratório de Radiocarbono, Instituto de Física, Universidade Federal Fluminense, Av. Litorânea s/n,
6 Niterói, RJ, Brazil.

7 ³Department of Ecology Swedish University of Agricultural Sciences, Ullsång 16 Uppsala, Sweden.

8

- 9 • Predicted radiocarbon distributions in open com part m e n t s i n a c c o r d i n g t o t h e
10 g a r o f o b e r t o n a n d m o d e l s
11 • Expected $\Delta^{14}\text{C}$ of ecosystem respiration are in accord with empirical $\Delta^{14}\text{C}$
12 d a t a
13 • Probability distributions of radiocarbon in open com part m e n t s p r o v i d e i n s i g h t s
14 i n t o e c o s y s t e m d y n a m i c s

15

Corresponding author: Ingrid Chanca, 

16
17
18
19
20
21
22
23
24
25
26
27
28

A
Radiocarbon (^{14}C) is commonly used as a tracer of the carbon cycle to determine how fast
carbon moves between different reservoirs such as plants, soils, reservoirs, oceans, and
the atmosphere. The mean lifetime (Δt) of an unknown probability distribution
function. We need a novel algorithm to compute Δt distributions from knowledge
of the age distribution of carbon in compartmental systems. One such
demonstrate the shape of the distributions might differ according to the speed of cy-
cling of components and their connectivity within the system, and are mostly
non-normal. The distributions are also sensitive to the variations of Δt in the atmosphere
over time, influenced by the changing anthropogenic effects of fossil-fuel emissions
(^{14}C -free) and nuclear weapons testing (bomb ^{14}C). Laboratory studies with
distributions can offer a simple and design of experiments aiming to capture the speci-
ficity of Δt in ecosystems.

29
30
31
32
33
34
35
36
37
38
39
40
41
42
43
44

Radiocarbon is a radioactive isotope of carbon prominent in environmental sciences for
tracking the dynamics of ecosystems especially as recent changes in atmospheric radiocar-
bon allow tracking excess ^{14}C created by weapons testing in the atmosphere on timescales
shorter than can be determined using radioactive decay. For climate change mitigation-
ation, a critical uncertainty is the time carbon captured through photosynthesis
in ecosystems before being released. For this reason, radiocarbon can be a valuable as a
biological tracer however it is necessary to accurately link the real age of carbon and its
radiocarbon age, as they usually differ. Forests and soils are open systems con-
necting compartments in natural systems differentiating timescales such as the mean age is
representing an age distribution that is not normally distributed. Here we develop an
algorithm to compute the ^{14}C content from modeling of multiple interconnected car-
bon pools. Our approach, offering an accurate estimate of the mean ^{14}C content of the
system and computation of the distribution of ^{14}C within the system at different points in
time. From the results we can have more insight into the dynamics of the carbon cycle and
how better design experiments to improve model-observations comparisons.

45 **1**

Radiocarbon (^{14}C) is a valuable tool for studying dynamical processes in living systems.
In particular, radiocarbon produced by nuclear bomb testing in the 1960s has been used in
many contexts as a tracer of the dynamics of carbon in different compartments of the
global carbon cycle, including the atmosphere, the terrestrial biosphere, and the oceans
(Godin et al., 1992; Jain et al., 1997; Randerson et al., 2002; Negler et al., 2006; Levin
et al., 2010). As a biological tracer, radiocarbon can be used to infer rates of carbon
cycling in specific compartments and to infer mean age in interconnected compartments.
Therefore, radiocarbon is used as a diagnostic metric to assess the performance of models of
the carbon cycle (Garn et al., 2017), and new data are being used to incorporate
radiocarbon in model benchmarking (Lawrence et al., 2020).

Carbon cycling in biological systems can be represented using a particular class of
mathematical model called compartmental systems (Sieni et al., 2018). As carbon enters
a system such as the terrestrial biosphere, it is stored and transferred among a network
of interconnected compartments such as soil age, wood, soils, and organisms.
Compartmental systems represent the dynamics of carbon as it circulates through the
compartments (Rasmussen et al., 2016; Sieni et al., 2018), and provides information about
the time carbon spends in particular compartments and the entire system (Rasmussen et
al., 2016; Sieni et al., 2017). Although these systems can be a direct application between the time
carbon spends in a compartmental system and its radiocarbon dynamics, several
both concepts

66 An open compartmental $\delta^{14}\text{C}$ contains information from (Jacob
 67 & Simons, 1993). The essential open compartmental $\delta^{14}\text{C}$ is analyzed by
 68 the concept of a *geand transit time* (Bolin & Rodhe, 1973; Rasmussen et al., 2016; Si en
 69 et al., 2017). In open $\delta^{14}\text{C}$ system, the incorporation and release of car
 70 bon occur continuously to define the concept of a *geand time elapsd*
 71 since carbon enters the compartmental $\delta^{14}\text{C}$ until a generic time. The *tra nsit time* can
 72 be defined as the time the carbon needs to travel through the entire $\delta^{14}\text{C}$, i. e., the time
 73 elapsd between carbon entry into the system.

74 In order to estimate the time mer of ^{14}C mean as a model linking both
 75 carbon and radiocarbon dynamics. Thompson and Randsen (1999) have
 76 implemented response functions from compartmental model to obtain ages and time
 77 independent radiocarbon dynamics. However, this approach is computationally pen-
 78 sive and can include numerical simulations are not long enough to cover the
 79 dynamics of slow mixing pools.

80 Explicit formulation and analysis of distributions in compartmental $\delta^{14}\text{C}$ have
 81 been recently developed (Meier & Si en, 2017). These formulations include nu
 82 merical models and can describe the age distributions of carbon for specific pool and
 83 for the entire compartmental $\delta^{14}\text{C}$. These age distributions give a radiocarbon in
 84 compartmental $\delta^{14}\text{C}$ system consists of a mixture of different $\delta^{14}\text{C}$, i. e., compartmental
 85 be described in terms of radiocarbon distributions at the relative proportion of
 86 carbon in a particular radiocarbon $\delta^{14}\text{C}$. However, until now radiocarbon is reported
 87 and modeled as a single quantity rather than the mean of an underlying distribution.

88 Knowledge of the distribution of ^{14}C obtained on the ^{12}C distribution (Cm as) in a
 89 compartmental $\delta^{14}\text{C}$ might give important insight on the model that better fits
 90 existing data. For example, by comparing the signal of radiocarbon in the pool and
 91 the relative vegetation signal in the pool model that describes the ecosystem.
 92 Consequently, empirical knowledge of the radiocarbon distribution of a particular $\delta^{14}\text{C}$, can
 93 play a significant role in determining the most appropriate model to describe a $\delta^{14}\text{C}$.

94 Model-data comparisons using radiocarbon are made more complex by the fact that
 95 atmospheric ^{14}C is continuously changing. This is particularly important for the 1960s
 96 when the nuclear bomb test began to age among the hemal network to the atmosphere,
 97 contributing to the formation of radiocarbon (bomb ^{14}C). In addition, large quantities of
 98 fossil-fuel derived carbon (^{14}C -free) have been emitted to the atmosphere, diluting the at
 99 mospheric radiocarbon signal and producing a false decline of radiocarbon $\delta^{14}\text{C}$ in recent
 100 years (Garn et al., 2017). Therefore, would expect a different radiocarbon distribution
 101 for every particular compartmental $\delta^{14}\text{C}$.

102 Obtaining a simple and accurate method to estimate radiocarbon distributions as a
 103 function of the year of observation is therefore, of great interest for experimental and
 104 modeling studies.

105 The main objective of this manuscript is to describe a method to obtain distributions
 106 of radiocarbon in compartmental $\delta^{14}\text{C}$ systems. In particular, we ask the fol-
 107 lowing research questions (i) How do distributions of radiocarbon change over time as a
 108 consequence of changes in atmospheric radiocarbon? (ii) How do empirical data compare
 109 to these conceptual radiocarbon distributions? (iii) What insights can these distributions
 110 provide for experimental and sampling design for improving model-data comparisons by
 111 capturing the entire variability of $\Delta^{14}\text{C}$ $\delta^{14}\text{C}$?

112 The manuscript is organized as follows. First, we provide the necessary theoretical
 113 background to obtain age and time distributions from compartmental $\delta^{14}\text{C}$ systems. Sec-
 114 ond, we describe an algorithm that computes radiocarbon distributions for particular $\delta^{14}\text{C}$
 115 using an age and time distributions and an atmospheric radiocarbon $\delta^{14}\text{C}$. Third,
 116 we present an application of our algorithm to a simple compartmental $\delta^{14}\text{C}$ adding the

117 each of us above. Finally, we discuss in the context of other applications
 118 and potential new insights from our approach.

119 **A**

120 **1**

121 Compartmental models describe the temporal dynamics of a system through
 122 a network of compartments and their transitions. A set of compartmental
 123 is characterized by a set of linear or nonlinear ordinary differential equations
 124 (ODE), whose solutions are the amount of material in each compartment at a certain time.

125 We will consider here linear autonomous compartmental models characterized by the
 126 mass of carbon at time t in compartment i as a vector $x(t)$. The mass of carbon in the
 127 compartment changes over time according to the following equation

128
$$\dot{x}(t) = Ax(t) + u, \quad x(0) = x_0 \quad (1)$$

129 where the vector u represents the input of carbon into the system, and the $n \times n$ com-
 130 partmental matrix A contains the diagonal entries representing the loss of carbon
 131 while the off-diagonal entries represent the transfer among them. In particular, the
 132 compartmental matrix in most compartmental models is a non-negative matrix reflecting
 133 the fact that the components (coefficients), representing the proportion of C trans-
 134 ferred from compartment i to compartment j and the decay rate k_i reflecting the loss of
 135 carbon from compartment i (rate $C_i k_i$) from any given compartment

136
$$A = \begin{pmatrix} -1 & 1 & 2 & \dots \\ 2 & 1 & -2 & \dots \\ \vdots & \vdots & \vdots & \ddots \\ 1 & 1 & 2 & \dots \end{pmatrix} \quad (2)$$

137 This matrix contains information on the dynamics, and size of a compartmental
 138 model. The net flux of carbon from the system can also be obtained from this matrix
 139 by summing all column elements, i.e., the output from a pool is a net loss of
 140 carbon from the system.

141 The information of the amount of carbon entering the system to be partitioned among
 142 the compartments is contained in the input vector

143
$$u = \begin{pmatrix} 1 \\ 2 \\ \vdots \end{pmatrix} \quad (3)$$

144 Linear autonomous systems of the form of equation (1) have an equilibrium point for
 145 each solution x^* given by

146
$$x^* = -A^{-1}u \quad (4)$$

147 where the mass of the compartments do not change over time, and inputs are equal to
 148 outputs of all compartments

1 49

A

1 50 Define age τ in a compartmental system as the time elapsed between the time of
 1 51 carbon entry into the generic time (Sierra et al., 2017). For a time-independent system
 1 52 in steady state, a probability distribution of ages of carbon in the compartment can be
 1 53 obtained using stochastic methods. According to Merand Sierra (2017), the vector of
 1 54 age densities for the compartment can be obtained as

$$1 55 \quad f_a(\tau) = (\mathbf{A}^{-1})^T \cdot \mathbf{A} \cdot \mathbf{u} \quad (5)$$

1 56 where $\mathbf{A} = \text{diag}(\lambda_1, \lambda_2, \dots, \lambda_n)$ is the diagonal matrix with the negative vector of
 1 57 carbon decay constants and \mathbf{A}^{-1} is the matrix exponential.

1 58 For the whole system, the age distribution is given by

$$1 59 \quad f_a(\tau) = -\mathbf{1}^T \cdot \mathbf{A} \cdot \mathbf{A}^{-1} \cdot \frac{\mathbf{x}}{\|\mathbf{x}\|} \quad (6)$$

1 60 where the symbol $\|\cdot\|$ represents the norm of the mass in a vector

1 61

1 62 Define τ_{inst} as the time elapsed since carbon enters the compartmental
 1 63 system until it leaves the boundaries of the system (Sierra et al., 2017). The τ_{inst} time
 1 64 is equivalent here to the age of the system. Merand Sierra (2017) also provide
 1 65 an explicit formula to obtain the τ_{inst} time density distribution for a time-independent
 1 66 system at steady state as

$$1 67 \quad f_{\tau_{\text{inst}}}(\tau) = -\mathbf{1}^T \cdot \mathbf{A} \cdot \mathbf{A}^{-1} \cdot \frac{\mathbf{u}}{\|\mathbf{u}\|} \quad (7)$$

1 68 These distributions are densities so they integrate to 1

$$1 69 \quad \int_0^{\infty} f_a(\tau) d\tau = \int_0^{\infty} f_{\tau_{\text{inst}}}(\tau) d\tau = 1 \quad (8)$$

1 70

1

1 72 We developed an algorithm to compute age and τ_{inst} time distributions in a $\Delta^{14}\text{C}$
 1 73 distribution for any given year of observation.

1 74 The algorithm consists in three main steps: 1) homogenization, 2) discretization, and 3)
 1 75 aggregation (Figure 1). We describe here the steps in detail in the sections below, using
 1 76 mathematical notation for the system age distribution, but concepts are similar for the
 1 77 τ_{inst} time distribution, and the age distribution of individual compartments.

1.1 Data

1 79 The main inputs for the algorithm are an age distribution $f_a(\tau)$, and an atmospheric
 1 80 radiocarbon concentration $\Delta^{14}\text{C}$ that provides the $\Delta^{14}\text{C}$ value of atmospheric CO_2 for a calendar
 1 81 year t . To homogenize the time scales of both $f_a(\tau)$ and $\Delta^{14}\text{C}$, we define the year of
 1 82 observation t_0 , as the year of interest to provide the radiocarbon distribution.

1 83 Since we are interested in determining the radiocarbon value of material observed in
 1 84 the system at time t_0 , we will look in the radiocarbon concentration $\Delta^{14}\text{C}$ in the past to obtain

1 85 he radiocarbon $\delta^{13}C$ in the $\delta^{13}C$ with an age t . Therefore, atmospheric radiocarbon
 1 86 can be expressed as a function of age, i. e., $(\delta^{13}C)_t = (\delta^{13}C)_0 - \lambda t$ (Figure 1). Both the
 1 87 $\delta^{13}C$ age distribution $P(\delta^{13}C)$ and the atmospheric radiocarbon $C(t)$ are functions
 1 88 of the continuous variable t at present age.

1 89 Several atmospheric radiocarbon datasets can be found in the literature (Reimer et al.,
 1 90 2013, 2020; Hogg et al., 2013, 2020; Hua et al., 2013; Levin et al., 1980; Levin & Komar
 1 91 1997; Levin et al., 2010; Gagnon et al., 2017). Also for cases of radiocarbon content in the
 1 92 atmosphere can be found in the recent literature (Gagnon, 2015; Sien, 2018). However,
 1 93 these atmospheric radiocarbon datasets do not necessarily have the same resolution in time.
 1 94 Some of them provide data at annual or form only time step, while
 1 95 in other datasets some are spaced by decades. To homogenize the resolution of the
 1 96 $\Delta^{14}C$ and to transform the radiocarbon dataset into a continuous function of t , we
 1 97 a cubic spline interpolation to obtain $\Delta^{14}C$ as a function of t . After this step, $C(t)$
 1 98 can be computed for any value of $t \in [0, \infty)$, and $C(t)$ will be a suitable data in the
 1 99 chosen radiocarbon atmospheric dataset.

2 00 t

2 01 Although we have now the age distribution and the radiocarbon data as continuous
 2 02 functions of age, we need to define these functions in intervals of size Δt . The reason
 2 03 for this discretization is that the probability density function of age $P(t)$ is a mean of
 2 04 the relative likelihood of an infinite small amount of mass having an age. But in a real
 2 05 world we need in the probability data small mass ascension radiocarbon distribution.
 2 06 Therefore, we need to define the probability density function to a probability mass
 2 07 function along a discrete variable $t \in [0, \infty)$. The new discrete probability function of
 2 08 ages can be defined as

$$2 09 \quad P(\Delta t) = \sum_{t=0}^{\infty} P(t) \Delta t \quad (9)$$

2 10 From this probability function, we can compute the position of total mass in the
 2 11 $\delta^{13}C$ with an age t as

$$2 12 \quad P(\Delta t) = \|x^*\| \quad (10)$$

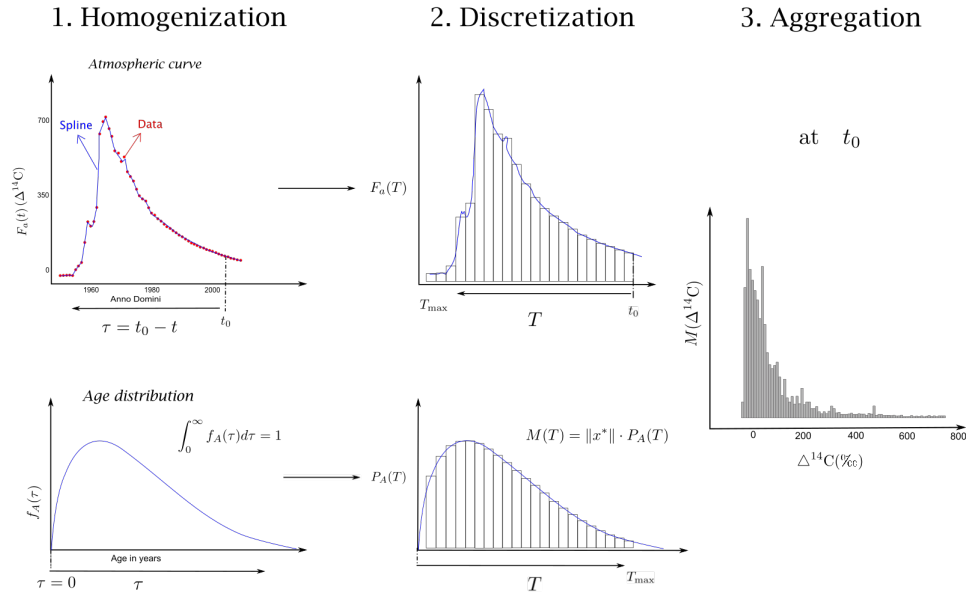
2 13 here

$$2 14 \quad \sum_{t=0}^{\infty} P(\Delta t) \approx 1 \quad (11)$$

$$\sum_{t=0}^{\infty} P(\Delta t) \neq \|x^*\|$$

2 15 Equation (11) implies that there is an approximation error by setting the continuous
 2 16 density function to a finite set of discrete intervals. This approximation error can be
 2 17 minimized by decreasing the size of the intervals and extending Δt as far as possible.

2 18 Once we define $P(\Delta t)$ to $P(t)$ and obtain discrete positions of mass with certain
 2 19 age t , we proceed to define the atmospheric radiocarbon $C(t)$ with respect to the
 2 20 same discrete interval of ages $t \in [0, \infty)$. This is simply done by computing $C(t) = C(t)$,
 2 21 which makes the assumption that in each interval $[t, t + \Delta t]$, the atmospheric radiocarbon
 2 22 value is equal to $C(t)$.



Graphical visualization of the three main steps for the computation of radiocarbon distributions in a compartmental system using an atmospheric radiocarbon curve of the carbon inputs to the systems, and the age distribution of carbon in a compartmental system. Details about each step are provided in the main text.

2 58

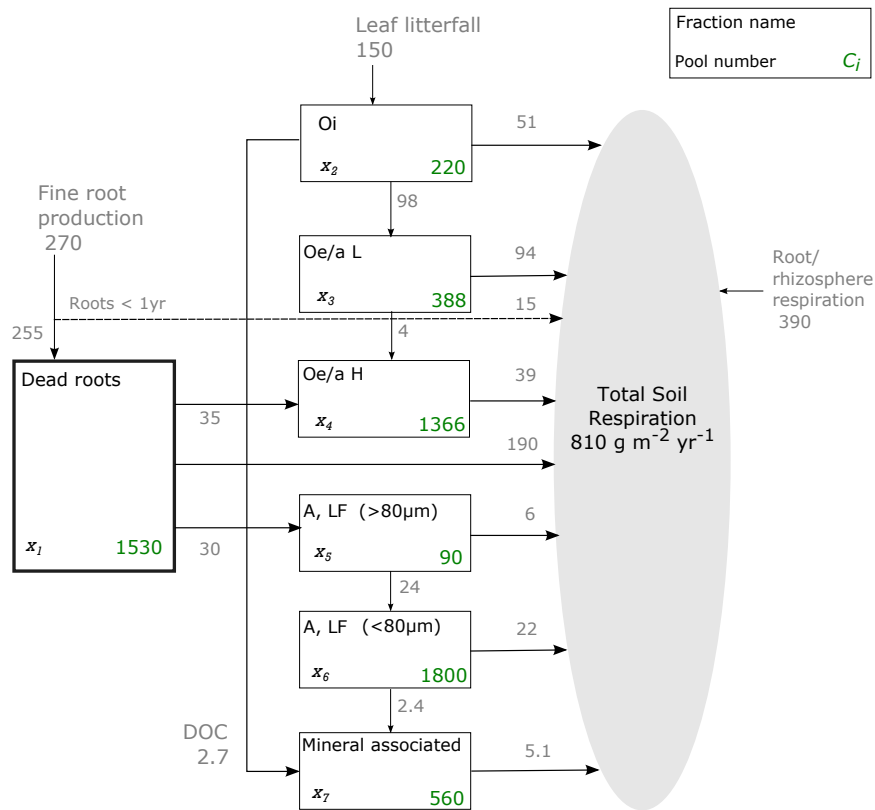
2 59 This approach can be used to obtain radiocarbon distributions for a near compartmental
 2 60 model of any representing carbon cycling process at different scales and for different
 2 61 biological systems.

2 62 We will focus here on a model that represents the dynamics of soil organic carbon
 2 63 at a temperate forest, which we call here in the Harvard Forest Soil (HFS) model. The
 2 64 model is based on measurements conducted at the Harvard Forest in Massachusetts, USA
 2 65 (Gardner et al., 2000; Siemann, Temmerman, et al., 2012). Soil samples collected in Ohio, OH,
 2 66 corresponding to 0–8 cm depth, and A-horizon (8–15 cm depth) were fractionated
 2 67 into seven soil fractions called: Dead Root C, Oe/a L, Oe/a H, A, IF (80 m),
 2 68 A, IF (80 m), and Mineral Associated. They were obtained as follows: The Ohio
 2 69 samples were divided after hand-picking into leaf litter (Oe/a L fraction), recognizable
 2 70 litter (Oe/a H fraction) and humified, i.e., organic matter that has been transformed by
 2 71 microbial action, corresponding to the fraction Oe/a H. Samples from the A-horizon were
 2 72 fractionated by density into low-density and high-density fractions. The high-density
 2 73 fraction corresponds to the Mineral Associated fraction. The low-density fraction is
 2 74 further divided by sieving into recognizable leaf litter (A, IF (80 m) fraction) and smaller than 80
 2 75 μm (A, IF (80 m) fraction). Details about the methodology used to fractionate the
 2 76 samples can be found in Gardner et al. (2000).

2 77 The compartmental model consists of seven pools (Figure 2); one pool corresponds
 2 78 to dead roots, P_1 , and the other pool corresponds to the different types of organic matter in
 2 79 the soil layer (O) called Oe/a L and Oe/a H, which correspond to pools P_2 , P_3 , and
 2 80 P_4 in the model. Two additional pools called A, IF (80 m), representing material from
 2 81 the A-horizon that floats in a dense (1 g cm⁻³) liquid and does not pass through an 80
 2 82 μm sieve and A, IF (80 m) (low-density fraction passing the sieve), represent the dynamics

of factors in the soil A horizon with different anion exchange capacity (Sierra and Trumbore, 2012).
 The soil pool 7 represents the dynamics of the mineral associated fraction (Sierra, Trumbore, et al., 2012).

The HFS model is built by fitting of empirical radiocarbon data from the above described samples. Details about the data to build the compartmental model are presented in Sierra, Trumbore, et al. (2012). For the same sites there are independent data (i.e., data not used for fitting the compartmental model) available. The independent data are in hisok consists of $\Delta^{14}\text{C}$ measurements on total soil CO_2 efflux collected in the year 1996, 1998, 2002, and 2008. The number of samples measured corresponding to the respective years is $n = 12$, $n = 28$, $n = 23$, and $n = 10$. With these data to compare the representativity of the mean $\Delta^{14}\text{C}$ measurements to the expected $\Delta^{14}\text{C}$ values obtained through our model.



Scheme of HFS model stocks () and fluxes among compartments (adapted from Sierra, Trumbore, et al. (2012)).

2 95 The form of ODE for the HFS model can then be expressed in compact form
 2 96 as

$$\begin{matrix}
 \cdot 1 & 255 & -2551530 & 0 & 0 & 0 & 0 & 0 & 0 & 0 & 1 \\
 \cdot 2 & 150 & 0 & -150220 & 0 & 0 & 0 & 0 & 0 & 0 & 2 \\
 \cdot 3 & 0 & 0 & 98152 & -98388 & 0 & 0 & 0 & 0 & 0 & 3 \\
 \cdot 4 & 0 & 35255 & 0 & 98 & -391366 & 0 & 0 & 0 & 0 & 4 \\
 \cdot 5 & 0 & 30255 & 0 & 0 & 0 & -3090 & 0 & 0 & 0 & 5 \\
 \cdot 6 & 0 & 0 & 0 & 0 & 0 & 2430 & -241800 & 0 & 0 & 6 \\
 \cdot 7 & 0 & 0 & 3152 & 0 & 0 & 0 & 25 & -5560 & 0 & 7
 \end{matrix}
 \quad (12)$$

2 98
 2 99 As described before, in order to estimate the radiocarbon distributions and expected
 300 values of $\Delta^{14}\text{C}$, the algorithm needs the following arguments: a compact matrix **A**,
 301 containing the decomposition and transfer within the pools; an input vector **u** con-
 302 taining the input as to be partitioned among the compartments; the year of obser-
 303 (equal to year of sampling in an experimental framework); the number of gas in the
 304 passive aim to compute the distributions for and a set of radiocarbon values in the at-
 305 mosphere, comprising the year of observation and the number of gas chosen. An additional
 306 argument is the distribution desired above, which has a default value of 0.1 gas
 307 but could be modified according to preferences

308 For the HFS model, **A** is the matrix in equation (12), with the form of equation (2),
 309 and **u** is the number vector in the same equation, with similar form as equation (3). We
 310 estimate the radiocarbon distributions of different types of observation, in order to address
 311 different research questions in this work. In the case of the passive distributions
 312 for the individual pools, total flux and volume km^3 , for the years 1965, 2027 and
 313 2100. Additionally in the *Supplementary Material* we provide the non-lagged radiocarbon
 314 distributions of individual pools, total flux and volume km^3 for the years 1950, 1965,
 315 2027, and 2100. Radiocarbon distributions of the outflux are presented for the years 1996,
 316 1998, 2002, and 2008, as for those gas values have independent $\Delta^{14}\text{C}$ data from oil
 317 CO_2 efflux compared to other measurements. For all those estimates the number of gas
 318 of computation was 1,000 gas. The bin size (‰) for plotting the histogram was set
 319 to 10 forms of the radiocarbon distributions except for the year 1965, where it was set
 320 to 40.

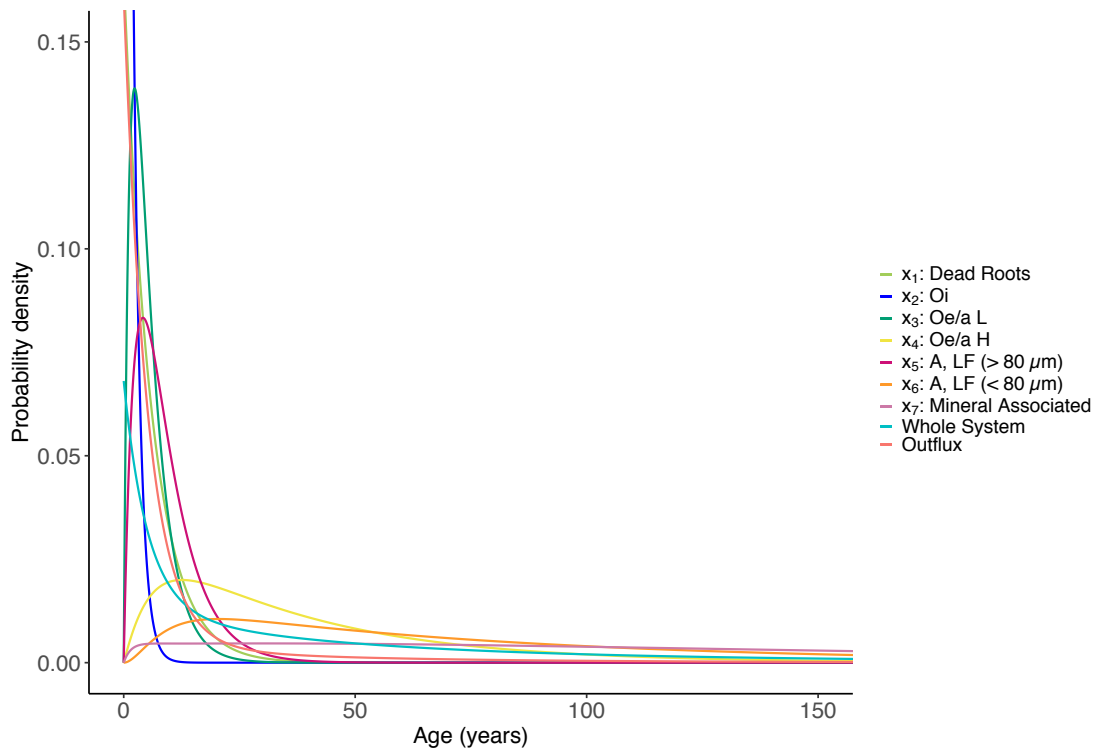
10

321
 322 The radiocarbon values for gas in the past e.g., AD 1965, were obtained by
 323 merging the recent year-based INCal 2.0 calibration curve (Reimer et al., 2020), which com-
 324 bines radiocarbon data and Bayesian statistical interpolation for the range 55,000–0 cal
 325 BP (BP = before present = AD 1950), and the records of atmospheric radiocarbon data
 326 compiled by Gagnon et al. (2017), from 1950 to 2015. Gagnon et al. (2017) also provides
 327 radiocarbon data in one-gas resolution on the range 1850 to 1949. However, since in this
 328 range the estimates were partially based on the previous Northern Hemisphere calibration
 329 curve (INCal 1.3, Reimer et al., 2013), we decided to use Gagnon et al. (2017)'s data set
 330 starting in AD 1950.

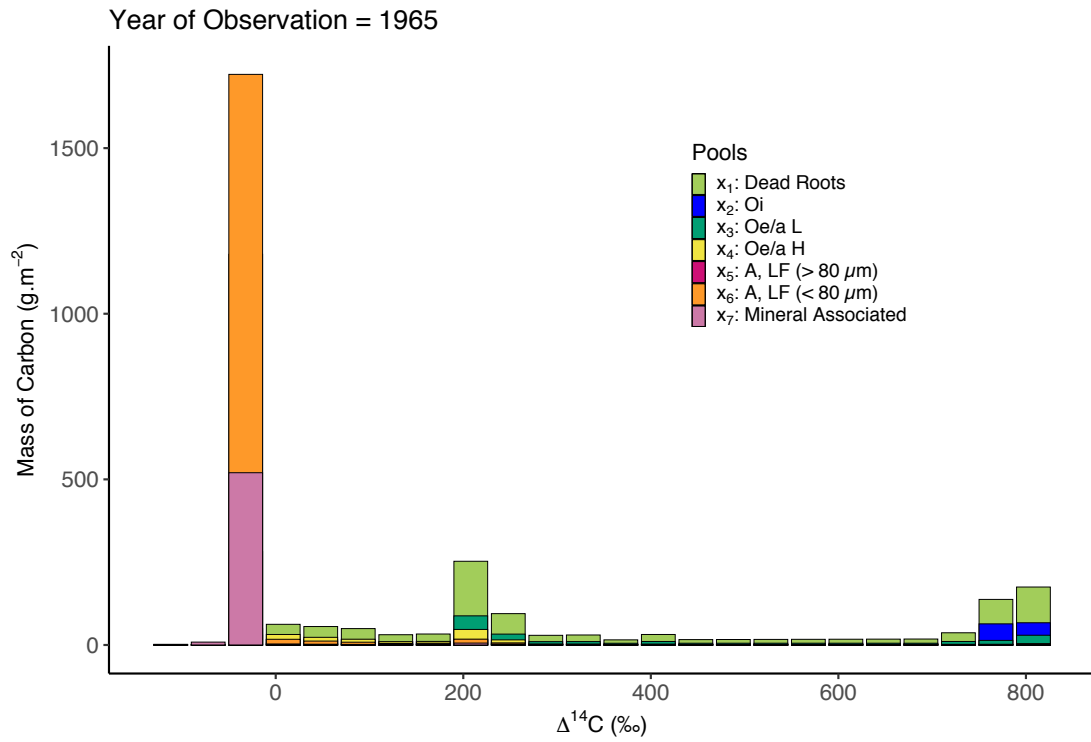
331 For the gas in the future, such as AD 2027 and 2100, we made use of the forecast
 332 estimates computed by Gagnon (2015), who simulated $\Delta^{14}\text{C}$ values in the atmosphere for
 333 four Representative Concentration Pathways of fossil fuel emissions: RCP2.6, RCP4.5, RCP6.0
 334 and RCP8.5. In this work we use the predictions based on the high emissions scenario
 335 (RCP8.5), starting in AD 2016.

33 as *Dead Roots* and *Oi*, most of the radiocarbon is nearly fixed around the recent
 34 atmospheric $\Delta^{14}\text{C}$ value in 2027, with almost no contributions from bomb ^{14}C .

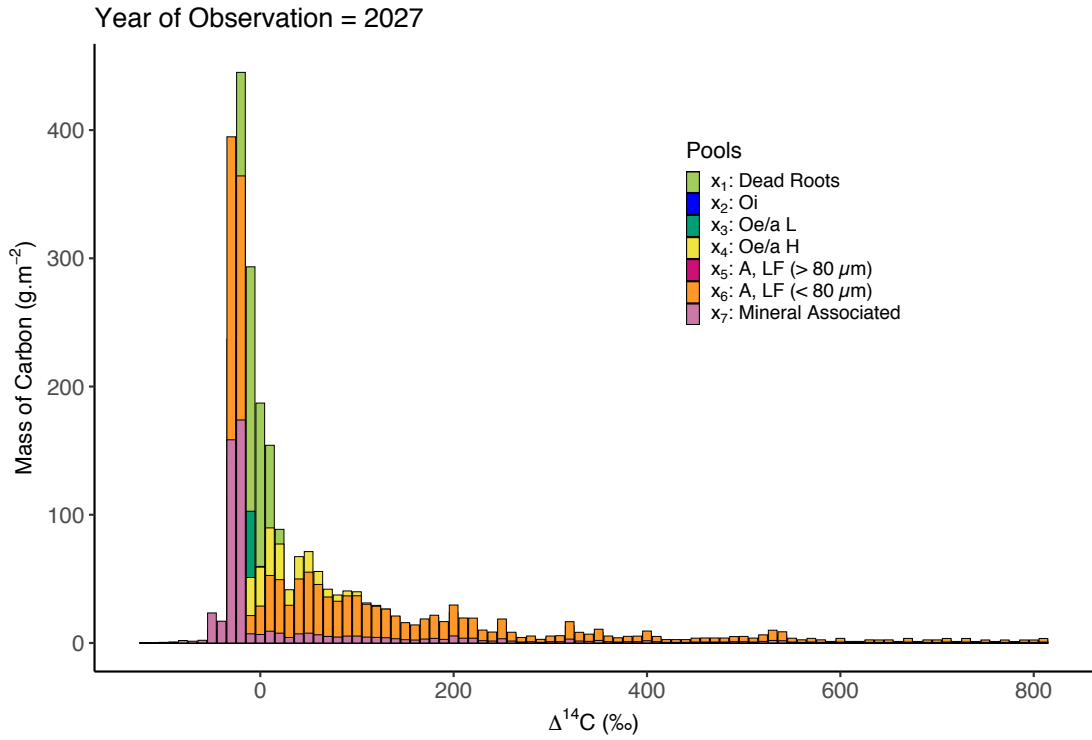
35 By the year 2100, the atmospheric $\Delta^{14}\text{C}$ will have dropped to -2.54 ± 0.5 ‰ (Garn,
 36 2015), reflecting the S effect. The distribution of most pools are less variable. For
 37 cycling pool share dropped to effect negative $\Delta^{14}\text{C}$ in the atmosphere over the 73 year
 38 since 2027, while the slow pools (*Mineral Associated*, *LF (> 80 μm)* and *Oe/a H* pool)
 39 still have a wide range of $\Delta^{14}\text{C}$ values at inclusion during the bomb period (now
 40 ~ 1.50 ‰ respectively).



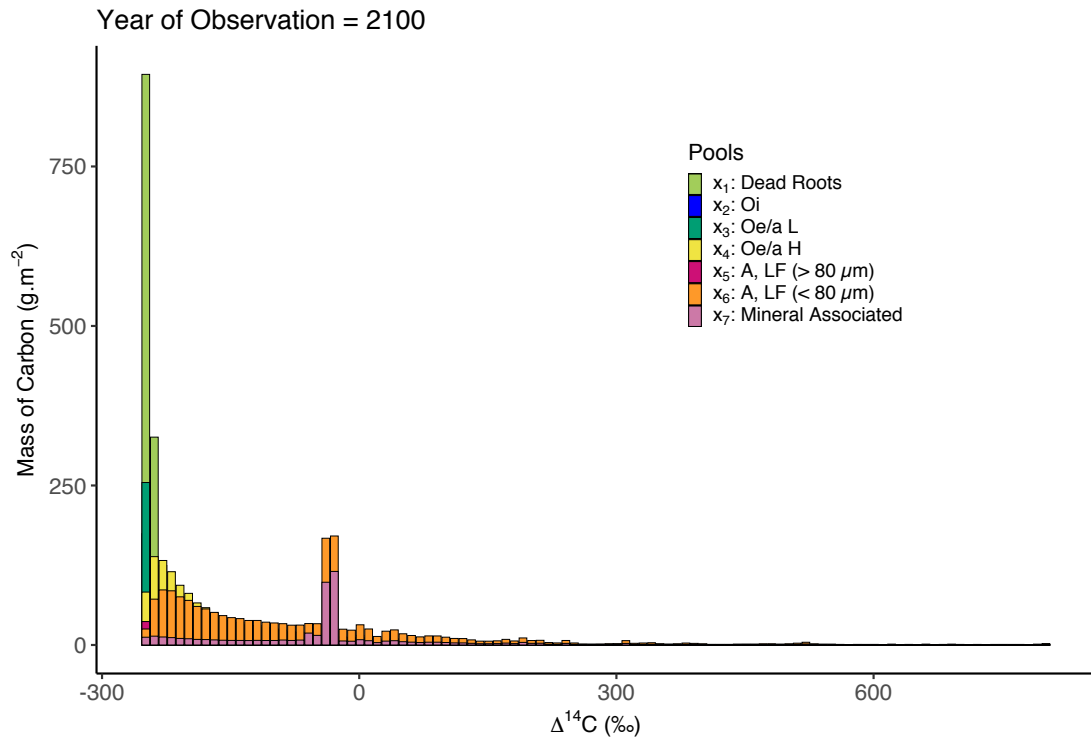
Age distributions for the Harvard Forest Soil model computed in a span of 1,000 years with a resolution of 0.1 year. The x-axis is limited to 150 years and the y-axis is limited to 0.15 for better visualization of the data.



$\Delta^{14}\text{C}$ distributions of each of the seven pools of the HFS model through the algorithm described above. The year of observation is 1965 – just after the bomb peak in 1964 – and the distributions are computed over 1,000 years. The bin size is equal to 40 ‰. The expected value and standard deviation of this distribution is 141 ± 280 .



$\Delta^{14}\text{C}$ distributions of each of the seven pools of the above-mentioned HFS model through the algorithm described above. The year of observation is 2027 and the distributions are computed over 1,000 years. The bin size is equal to 10 ‰. The expected value and standard deviation of this distribution is 54 ± 144 .



$\Delta^{14}\text{C}$ distributions of each of the seven pools of the above-mentioned HFS model through the algorithm described above. The year of observation is 2100 and the distributions are computed over 1,000 years. The bin size is equal to 10 ‰. The expected value and standard deviation of this distribution is -147 ± 146 .

Figure 7. $\Delta^{14}\text{C}$ distributions of *Outflux* and *Whole System* of the HFS model for the years 1965, 2027 and 2100. The bin size \mathbf{b} for all the three years is equal to 40 h .

Figure 8. Evolution of the expected $\Delta^{14}\text{C}$ values of *Outflux* and *Whole System* for the HFS model between the years 1900 and 2100.

Table 1. ^{14}C ranges with the highest masses of radiocarbon according to our estimations; ^{14}C expected values according to weighted mean of mass distribution of radiocarbon; and observed ^{14}C mean values of soil CO_2 e ux.

^{14}C [h]					
Year	Primary Peaks ^a	Secondary Peaks ^b	Expected value ^c	Mean value ^d	
1996	(112, 122]	(-28, -18], (102, 112], (122, 212]	153 107.6	129.5	17.3
1998	(-37, -17], (93, 153]	(153, 273], (323, 333], (493, 503]	139.4103.3	117.6	26.2
2002	(82, 102]	(-28,-18], (72, 82], (102, 152]	115.9 96.3	100.8	8.4
2008	(51,61]	(41, 51], (61, 121], (-29, -19]	85 89.7	74.8	13.6

a For 1996, 2002 and 2008, masses 10^3 g m^{-2} ; For 1998, masses 10^2 g m^{-2} ;

b For 1996, 2002 and 2008, masses 10^2 g m^{-2} ; For 1998, masses 10 g m^{-2} ;

c Expected value of theoretical radiocarbon distribution of the Out ux (weighted mean);

d Mean value of the ^{14}C values measured on soil CO_2 e ux from the Harvard Forest.

Figure 9. Comparison between theoretical radiocarbon distribution and independent empirical data. a: Year of observation equals to AD 1996; b: Year of observation equals to AD 1998; c: Year of observation equals to AD 2002; d: Year of observation equals to AD 2008.

time distributions from compartmental systems should be able to answer a number of
 questions about the compartmental model dynamics.

More recently, Gadnik et al. (2000), limited information about the
 cycling rates obtained by ^{14}C measurements of bulk SOM made at a single point in
 time. Therefore, being able to compare radiocarbon distributions for different
 observations could improve the interpretation of the evolution of soil radiocarbon in
 terms of carbon dynamics.

52 0

Compartmental models are a common approach to describe the dynamics of open
 systems. When modeling the carbon cycle in ecosystems, the main mathematical equ-
 ations developed to obtain age and distribution are a set of ordinary differential
 equations in state space, and here we use the compartmental model to obtain radiocarbon dis-
 tributions in the same system as a powerful method. The algorithm presented, besides
 being simple, demonstrates the potential power of the method. It also shows how a
 specific model, predictions can be compared with experimental data.

Radiocarbon distributions can be obtained with the knowledge of atmospheric
 $\Delta^{14}\text{C}$ and the model of the change in radiocarbon in each compartment and isotopes
 over a period of decades. This provides a powerful method to
 estimate the radiocarbon distribution and the model of carbon dynamics in soils
 and ecosystems.

Our study shows how the heterogeneity of the ecosystem is described through
 the mixing of material in the pool and the age of the radiocarbon distributions.
 As opposed to age and distribution of material in each state, radiocarbon
 distributions are expected to vary in time, being dependent on the carbon observation
 as a consequence of the dependence on the atmospheric ^{14}C input in the system. This
 non-linear distribution is a possible change according to the carbon observation, but it
 is expected to be smooth and a priori.

All factors influencing pool size and heterogeneity present in a specific pool are
 of observations in a specific pool as well as the heterogeneity of compartments
 present in a specific pool and multiple peaks of $\Delta^{14}\text{C}$ for high labeled gas (e.g., 1965, when
 the concentration of ^{14}C in the atmosphere was almost twice the natural
 level).

The theoretical distributions can be estimated for specific time points over which
 not all are feasible in experiments. The atmospheric concentration through the algorithm has
 to be taken care of when one aims to compare them to empirical data. It is also important
 to be aware of the radiocarbon atmospheric level and the distribution as the
 variation of atmospheric $\Delta^{14}\text{C}$ can influence the age and mean age of the distributions.
 In this sense, having accurate data on the ^{14}C concentration in the atmosphere is
 a key factor in the determination of the radiocarbon distribution in multiple interconnected
 systems.

553 A

The authors would like to thank Ingeborg Leiv for her meaningful comments and sug-
 gestions on this work. This work is supported by the scientific research developed at
 the Amazon Tall Tower Observatory (ATTO), which is supported by the German Fed-
 eral Ministry of Education and Research (grant number 01 IK1602A) and the Max Planck
 Society.

The atmospheric $\Delta^{14}\text{CO}_2$ datasets in his research are available through Gaen (2015), Gaen et al. (2017), and Reimer et al. (2020). Data on the compartmental model presented in his research, including the independent $\Delta^{14}\text{C}$ data set for comparison with other measurements are available through Si et al., Tmboe, et al. (2012).

References

- Bolin, B., & Rodhe, H. (1973). A note on the concept of age distribution and transition time in natural reservoirs. *Tellus*, 25(1), 58-62.
- Gadnki, J. B., Tmboe, S. E., Davidson, E. A., & Zeng, S. (2000). Soil carbon cycling in a temperate forest: a carbon-based estimate of residence time separation and partitioning of fluxes. *Biogeochemistry*, 51(1), 33-69.
- Godin, J. (1992). Biosphere carbon sequestration potential and the atmospheric ^{14}C carbon cycle. *Journal of Experimental Botany*, 3(8), 1111-1119.
- Gaen, H. D. (2015). Impact of fossil fuel emissions on atmospheric radiocarbon and its application to radiocarbon ocean sciences. *Proceedings of the National Academy of Sciences*, 112(31), 9542-9545.
- Gaen, H. D., Allison, C. E., Ehrig, D. M., Hammer, S., Keeling, R. F., Levin, I., . . . others (2017). Compiled records of carbon isotopes in atmospheric CO_2 for historical simulation. *Geoscientific Model Development (Online)*, 10(12).
- Hogg, A. G., Heath, T. J., Hua, Q., Palmer, J. G., Toney, C. S., Solomon, J., . . . others (2020). Shal 2018 in hemispheric calibration, 055,000 gascal bp. *Radiocarbon*, 62(4), 759-778.
- Hogg, A. G., Hua, Q., Blackwell, P. G., Nium, B., Cook, C. E., Guilderson, T. P., . . . others (2013). Shal 13 in hemispheric calibration, 050,000 gascal bp. *Radiocarbon*, 55(4), 1889-1903.
- Hua, Q., Baret, M., & Rakowski, A. Z. (2013). Atmospheric radiocarbon for the period 1950-2011. *Radiocarbon*, 55(4), 2059-2072.
- Jacobs, J. A., & Simon, C. P. (1993). Climate history of compartmental systems. *Science*, 260(5111), 437-9.
- Jain, A. K., Khosravi, H. S., & Woelke, D. J. (1997). Is there an imbalance in the global budget of bomb-produced radiocarbon? *Journal of Geophysical Research: Atmospheres*, 102(D1), 1327-1333.
- Lance, C. R., Beem-Miller, J., Hoy, A. M., Moore, G., Si et al., C. A., Heckman, K., . . . others (2020). An open source database for the analysis of soil radiocarbon data: IADON 1.0. *Earth System Science Data*, 12(1), 1-12.
- Levin, I., & Komar, B. (1997). Trends of atmospheric ^{14}C observations at sea level and at sea level. *Radiocarbon*, 49(2), 205-218.
- Levin, I., Mich, K., & W. W. (1980). The effect of anthropogenic CO_2 and ^{14}C on the distribution of ^{14}C in the atmosphere. *Radiocarbon*, 22(2), 379-391.
- Levin, I., Negler, T., Komar, B., Diehl, M., Fancey, R., Gomez-Lopez, A., . . . Why, D. (2010). Observations and modeling of the global distribution and long-term trend of atmospheric ^{14}C . *Tellus B: Chemical and Physical Meteorology*, 62(1), 26-46.
- Meyer, H., & Si et al., C. A. (2017, July). A near-atmospheric compartmental model as a constraint on the transition time and age distributions. *Mathematical Geosciences*, 50(1), 1-34. Retrieved from <https://doi.org/10.1007/s11004-017-9690-1> doi: 10.1007/s11004-017-9690-1
- Negler, T., Ciais, P., Rodhe, K., & Levin, I. (2006). Exchange of radiocarbon constraints on air-sea exchange and the uptake of CO_2 by the oceans. *Geophysical Research Letters*, 33(11).
- Randerson, J., Enting, I., Schimel, D., Caldeira, K., & Fung, I. (2002). Seasonal and latitudinal variability of atmospheric ^{14}C : Bomb contributions from fossil fuel oceans to the atmosphere, and the terrestrial biosphere. *Global Biogeochemical Cycles*, 16(4).

- 611 Rasmussen, M., Hastings, A., Smith, M. J., Agosto, F. B., Chen-Charpentier, B. M., Ho -
 612 man, F. M., ... others (2016). Transit times and mean ages for nonautonomous
 613 and autonomous compartmental systems. *Journal of mathematical biology*, 73(6-7),
 614 1379{1398.
- 615 Reimer, P. J., Austin, W. E., Bard, E., Bayliss, A., Blackwell, P. G., Ramsey, C. B., ...
 616 others (2020). The intcal20 northern hemisphere radiocarbon age calibration curve
 617 (0{55 cal kbp). *Radiocarbon*, 62(4), 725{757.
- 618 Reimer, P. J., Bard, E., Bayliss, A., Beck, J. W., Blackwell, P. G., Ramsey, C. B., ... others
 619 (2013). Intcal13 and marine13 radiocarbon age calibration curves 0{50,000 years cal
 620 bp. *Radiocarbon*, 55(4), 1869{1887.
- 621 Santos, G. M., Oliveira, F. M., Park, J., Sena, A. C., Chiquetto, J. B., Macario, K. D.,
 622 & Grainger, C. S. (2019). Assessment of the regional fossil fuel co2 distribution
 623 through 14c patterns in ipê leaves: The case of rio de janeiro state, brazil. *City and
 624 Environment Interactions*, 1, 100001.
- 625 Sierra, C. (2018). Forecasting atmospheric radiocarbon decline to pre-bomb values. *Radiocarbon*,
 626 60(4), 1055{1066.
- 627 Sierra, C., Ceballos-Núñez, V., Metzler, H., & Müller, M. (2018). Representing and un-
 628 derstanding the carbon cycle using the theory of compartmental dynamical systems.
 629 *Journal of Advances in Modeling Earth Systems* 10(8), 1729{1734.
- 630 Sierra, C., Müller, M., Metzler, H., Manzoni, S., & Trumbore, S. (2017). The muddle of
 631 ages, turnover, transit, and residence times in the carbon cycle. *Global change biology*
 632 23(5), 1763{1773.
- 633 Sierra, C., Müller, M., & Trumbore, S. (2014). Modeling radiocarbon dynamics in soils:
 634 Soilr version 1.1. *Geoscientific Model Development* 7(5), 1919{1931.
- 635 Sierra, C., Müller, M., Trumbore, S., et al. (2012). Models of soil organic matter decomposi-
 636 tion: the soilr package, version 1.0. *Geoscientific Model Development* 5, 1045{1060.
- 637 Sierra, C., Trumbore, S., Davidson, E., Frey, S., Savage, K., & Hopkins, F. (2012). Pre-
 638 dicting decadal trends and transient responses of radiocarbon storage and fluxes in a
 639 temperate forest soil. *Biogeosciences* 9(8), 3013{3028.
- 640 Stuiver, M., & Polach, H. A. (1977). Discussion reporting of 14 c data. *Radiocarbon*, 19(3),
 641 355{363.
- 642 Suess, H. E. (1955). Radiocarbon concentration in modern wood. *Science*, 122(3166),
 643 415{417.
- 644 Thompson, M. V., & Randerson, J. T. (1999). Impulse response functions of terrestrial
 645 carbon cycle models: method and application. *Global Change Biology* 5(4), 371{
 646 394.